Approximate Method for the Calculation of Nonequilibrium Radiative Heat Transfer

Robert B. Greendyke*
Analytical Services and Materials, Inc., Hampton, Virginia 23666
and
Lin C. Hartung†
NASA Langley Research Center, Hampton, Virginia 23665

A simplified method for the calculation of radiative heat transfer in hypersonic re-entry flows where local thermal nonequilibrium (LTNE) conditions exist is presented. This method has been incorporated into the computer code RADMC (Radiation/Modified Corrections), which utilizes an approximate "two-state" model of the electronic levels of atoms and molecules in the determination of the populations of the excited states for both LTNE and local thermal equilibrium (LTE) conditions for each of the relevant chemical species. The population data are used to calculate a correction factor to the radiative cross sections in an eight-step nongray radiative heat transfer model. Uncoupled results have been obtained for various points along the proposed trajectory of the Aeroassist Flight Experiment and the Fire II trajectory, and compared with results obtained for the same flowfields from the Nonequilibrium Air Radiation (NEQAIR) radiative heat-transfer code.

Nomenclature

AEX	= atomic excitation energy, erg
D	= dissociation energy, erg
g	= degeneracy of particle state
h	= Planck constant, erg-s
I	= ionization energy, erg
IR	= infrared portion of the spectrum
k	= Boltzmann constant, erg/K
m	= mass of a particle, g
MEX	= molecular excitation energy, erg
N	= number density, particles/cm^3
Q	= partition function
UV	= ultraviolet portion of the spectrum
VIS	= visible portion of the spectrum
VUV	= vacuum ultraviolet portion of the spectrum
1	= ground state
2	= excited state
α	= atomic correction factor
β	= molecular correction factor
ϵ	= energy, erg
θ	= characteristic temperature

Subscripts

act	= actual
e	= electron
el	= electronic
h	= heavy particle
LTE	= local thermal equilibrium
LTNE	= local thermal nonequilibrium
r, rot	= rotation
spin	= electron spin
tr	= translation
v, vib	= vibration

Presented as Paper 90-0135 at the AIAA 28th Aerospace Sciences Meeting, Reno, NV, Jan. 8-11, 1990; received Feb. 11, 1990; revision received June 25, 1990; accepted for publication July 2, 1990.

*Research Scientist. Member AIAA.
†Aerospace Engineer. Member AIAA.

Introduction

IN the near future, the Aeroassist Flight Experiment (AFE)[1,2] will be conducted to test the concept of aerocapture for future space vehicles. At the high altitudes of its planned trajectory, the AFE will be in a highly rarefield flowfield regime where chemical and thermal nonequilibrium effects will dominate the flow. The nonequilibrium conditions will significantly influence the radiative heat transfer.

Thermal nonequilibrium presents a problem in most radiative heat transfer models, particularly in nongray step models. Most of the radiation step models obtain the spectral absorption coefficient by multiplying the number density of the radiating chemical species by a radiative cross section appropriate for local thermal equilibrium (LTE) conditions. Inherent in the definition of a radiative cross section is a ratio of the population of the excited states of the species to the total population of the species under consideration. This ratio, whether the cross section is obtained by empirical observation or quantum mechanics, is obtained by assuming a Boltzmann distribution of particles through their energy levels, However, at local thermal nonequilibrium (LTNE) conditions, such an equilibrium distribution will not be present. In order to obtain accurate estimates of the radiative heat transfer in a nonequilibrium flow regime, the radiative cross sections need to be corrected for this situation.

Previous work by Carlson et al.[1] and Greendyke[3] had indicated that the modification of cross sections could be accomplished for the eight-step model of equilibrium air radiation, originally developed by Olstad,[4] with little computational difficulty. Unfortunately, when this modified method was applied to a viscous flowfield solution, the method broke down in the low-temperature environment of the boundary layer where thermal nonequilibrium was at a minimum, yet chemical nonequilibrium effects were present. The previous method had focused on finding a correction factor that corrected the radiative cross sections for chemical as well as thermal nonequilibrium. In the present work, it is assumed that the

radiative cross sections need to be corrected for thermal nonequilibrium effects alone, and that chemical nonequilibrium will be accounted for through the species number densities resulting from the chemical kinetics of the flowfield solution method. In addition, all radiative heating calculations in this study are performed in an uncoupled fashion from the flowfield solution. Therefore, this paper presents an alternative approximate method of obtaining the correction factors, which is well-behaved throughout the flowfield and is computationally efficient, and compares the results of this method to those of an existing code Nonequilibrium Air Radiation (NEQAIR)[5] as well as to experimental data from the Fire II experiment.

Nonequilibrium Correction Factors

In order to simplify the calculation of the population of the excited states for the atoms and molecules present in a flowfield, the assumption of a "two-state" model of excitation is made. The two-state model assumes that the upper electronic levels of both atoms and molecules can be compressed into a single excited state. Any low-energy levels can be similarly compressed into one ground state. The particle under consideration would then have a single ground state and an excited state. This, of course, implies the compression of the vibrational levels for the diatomic species as well. The energy of the excited state is then

$$\epsilon(2) = \frac{\Sigma g_j \epsilon_j}{\Sigma g_j} \tag{1}$$

where the summation is carried out over the upper electronic levels, and the degeneracy of the excited state is simply

$$g(2) = \Sigma g_j \tag{2}$$

The electronic levels for the particles can be schematically represented as shown in Fig. 1.

The assumption was made, and later checked (Table 1), that the energy difference between the excited molecular state and the ground atomic state, as well as the energy difference between the excited atomic state and the ground ionic state, would be small compared with the differences between the ground and excited energy levels, or

$$(D - \epsilon_{MEX}) \ll \epsilon_{MEX}$$

$$(I - \epsilon_{AEX}) \ll \epsilon_{AEX}$$

In LTNE, a Boltzmann distribution cannot be assumed to exist between the various electronic levels for a given chemical species, yet the assumption that a Boltzmann distribution exists somewhere is necessary to calculate the excited state populations needed for radiation calculations in this regime. Therefore, given the small energy difference between the excited atomic state and the ground ionic state in the two-state model, few energy exchange processes would be required to equilibrate these two states, and if a Boltzmann distribution could be assumed to exist anywhere, it would be between these two states. The reaction can be expressed as

$$N(2) \rightleftarrows N^+ + e^-$$

and in the case of nitrogen and for oxygen as

$$O(2) \rightleftarrows O^+ + e^-$$

The use of statistical mechanics is assumed to derive a formula in terms of partition functions for the calculation of the population of the excited states at LTNE and LTE conditions. For LTNE

$$\frac{N_{\text{LTNE}}^{N(2)}}{N_{\text{act}}^{N^+} N_{\text{act}}^{e^-}} = \frac{Q_{\text{el}}^{N(2)} Q_{\text{tr}}^{N(2)}}{Q_{\text{el}}^{N^+} Q_{\text{tr}}^{N^+} Q_{\text{spin}}^{e^-} Q_{\text{tr}}^{e^-}} \exp(I/kT_1) \tag{3}$$

this study assumes that

$$T_1 = \sqrt{T_e T_h}$$

The second term on the right side of Eq. (3) represents the normalization of the ionic ground state to that of the atomic ground state. In the ionization reactions of all the chemical kinetics models for this study, some ions are formed through heavy particle collisions that are dominated by the heavy particle temperature T_h, and some ions are formed by electron impact reactions that are dominated by the electron temperature T_e. Therefore, the use of the geometrically averaged temperature is believed to be correct in the normalization of the energy levels of the atomic state to the ionic state. The actual number density of excited nitrogen atoms for LTNE can then be found through expanding the partition functions as

$$N_{\text{LTNE}}^{N(2)} = \frac{N_{\text{act}}^{N^+} N_{\text{act}}^{e^-}}{2} \left[\frac{h^2}{2\pi m_e k T_e}\right]^{3/2} \times \left[\frac{g^{N(2)}_{(2)} \exp(-\epsilon_{AEX}^{N(2)}/kT_e)}{\sum_j g_j^{N^+} \exp(-\epsilon_j^{N^+}/kT_e)}\right] \exp(I/kT_1) \tag{4}$$

The actual number density of ground state nitrogen atoms can then be found simply from

$$N_{\text{LTNE}}^{N(1)} = N_{\text{total}}^{N} - N_{\text{LTNE}}^{N(2)} \tag{5}$$

The previous discussion can be applied to the calculation of excited state populations at LTE conditions. In LTE conditions, the various modes of energy will tend to equilibrate with

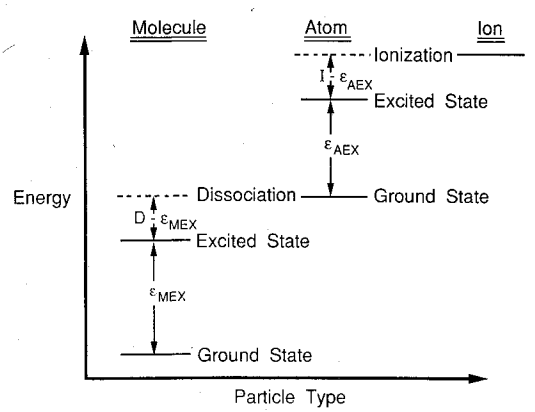

Fig. 1 Schematic representation of energy levels.

Table 1 Particle energy levels

Particle	State	g	ϵ (erg)
O	1	15	1.5075×10^{-12}
	2	3,140	2.1302×10^{-11}
	Ion	—	2.1813×10^{-11}
N	1	20	3.6281×10^{-12}
	2	6,840	2.2807×10^{-11}
	Ion	—	2.3304×10^{-11}
O_2	1	6	9.5632×10^{-13}
	2	4	7.1187×10^{-12}
	D	—	8.2142×10^{-12}
N_2	1	1	0.0
	2	11	1.1612×10^{-11}
	D	—	1.5600×10^{-11}

the translational mode of energy. One can then calculate excited state populations in LTE by using Eqs. (4) and (5) and simply replacing the various temperatures by the heavy particle translational temperature. Using atomic nitrogen as an example again

$$N_{\mathrm{LTE}}^{N(2)} = \frac{N_{\mathrm{act}}^{N^+} N_{\mathrm{act}}^{e^-}}{2} \left[\frac{h^2}{2\pi m_e k T_h}\right]^{3/2} \times \left[\frac{g_{(2)}^{N(2)} \exp(-\epsilon_{AEX}^{N(2)}/kT_h)}{\sum_j g_j^{N^+} \exp(-\epsilon_j^{N^+}/kT_h)}\right] \exp(I/kT_h) \tag{6}$$

and

$$N_{\mathrm{LTE}}^{N(1)} = N_{\mathrm{total}}^{N} - N_{\mathrm{LTE}}^{N(2)} \tag{7}$$

The correction factor used in the radiative heat transfer for atomic nitrogen processes is then

$$\alpha_N = N_{\mathrm{LTNE}}^{N(2)}/N_{\mathrm{LTE}}^{N(2)} \tag{8}$$

An identical argument can be made for atomic oxygen, resulting in the correction factor for atomic oxygen processes being

$$\alpha_O = N_{\mathrm{LTNE}}^{O(2)}/N_{\mathrm{LTE}}^{O(2)} \tag{9}$$

The denominator in Eqs. (8) and (9) could be determined by the use of a Boltzmann distribution function. However, using such a distribution implies both thermal and chemical equilibrium and produces errors in the boundary layer that are identical to the errors resulting from the original formulation of the correction factors.[1] In the current approach, a correction factor is sought for thermal nonequilibrium alone. Use of a Boltzmann distribution also corrects for chemical nonequilibrium and is therefore not appropriate.

The small energy difference between the excited molecular state and the ground atomic state again allows the assumption of a Boltzmann distribution between the two. The resulting chemical reaction is

$$N_2(2) \rightleftharpoons 2\,N(1)$$

or for diatomic oxygen

$$O_2(2) \rightleftharpoons 2\,O(1)$$

Again, the assumption is made that the nitrogen reaction can be expressed, in terms of partition functions, as

$$\frac{N_{\mathrm{LTNE}}^{N_2(2)}}{\left[N_{\mathrm{act}}^{N(1)}\right]^2} = \frac{Q_{\mathrm{tr}}^{N_2(2)} Q_{\mathrm{el}}^{N_2(2)} Q_{\mathrm{vib}}^{N_2(2)} Q_{\mathrm{rot}}^{N_2(2)}}{\left[Q_{\mathrm{tr}}^{N(1)} Q_{\mathrm{el}}^{N(1)}\right]^2} \exp(D/kT_2) \tag{10}$$

where, for this study,

$$T_2 = \sqrt{T_v T_h}$$

Table 2 Eight-step air radiation model

Band	Wavelength, Å	Wavelength, ev	Spectral range
1	400- 852	14.56-31.00	VUV continuum
2	852- 911	13.62-14.56	VUV continuum
3	911-1020	12.16-13.62	VUV continuum
4	1020-1130	10.98-12.16	VUV continuum
5	1801-4000	3.10- 6.89	"Visible"
6	1130-1801	6.89-10.98	Continuum + line wings
7	1130-1801	6.89-10.98	Line "centers"
8	4000- ∞	0. - 3.10	Visible + infrared

The geometric average of vibrational temperature and heavy particle temperature was used as the normalizing temperature in this situation to reflect that dissociation is a process of both heavy particle collision and vibrational excitation. The actual excited state population of diatomic nitrogen is then

$$N_{\mathrm{LTNE}}^{N_2(2)} = \left[N_{\mathrm{act}}^{N(1)}\right]^2 \sqrt{2} \left[\frac{h^2}{2\pi m_N k T_h}\right]^{3/2} \times \left[\frac{g_{(2)}^{N_2(2)} \exp(-\epsilon_{MEX}^{N_2(2)}/kT_e)}{g_{(1)}^{N(1)} \exp(-\epsilon_{(1)}^{N(1)}/kT_e)}\right] \times \frac{1}{[1 - \exp(-\theta_{\mathrm{vib}}^{N_2}/T_v)]} \left(\frac{T_h}{\theta_r^{N_2}}\right) \exp(D/kT_2) \tag{11}$$

where the actual number density of ground state atomic nitrogen was found in the determination of the atomic correction factors. The number density of ground state diatomic nitrogen can be found by a similar method as in Eqs. (5) and (7), but it is unnecessary in determining the molecular correction factors.

The population of excited diatomic nitrogen at LTE conditions can be determined by replacing all the temperatures in Eq. (11) with the heavy particle translational temperatures, as in Eq. (6). The correction factor for diatomic nitrogen radiative process is then expressed as

$$\beta_N = N_{\mathrm{LTNE}}^{N_2(2)}/N_{\mathrm{LTE}}^{N_2(2)} \tag{12}$$

Using identical logic, the correction factor for diatomic oxygen processes is found to be

$$\beta_O = N_{\mathrm{LTNE}}^{O_2(2)}/N_{\mathrm{LTE}}^{O_2(2)} \tag{13}$$

It is important to note that in thermal equilibrium all correction factors will be equal to one by definition. In this case, the radiative cross sections receive no correction, and the model is identical to the original model of Olstad.[4] The actual incorporation of the correction factors into the eight-step model is identical to the method of Carlson et al.,[1] and the spectral range of the model can be seen in Table 2.

Results

For the purposes of this investigation, only the stagnation streamline radiative fluxes are studied. The flowfield solution methods used are based on a two-temperature model (T_h and T_{vib}), whereas the RADMC (Radiation/Modified Correction) and NEQAIR[5] codes were originally written to utilize three temperatures. The assumption was made for this study that $T_e = T_{\mathrm{vib}}$. Freestream conditions for the AFE and Fire II points examined are listed in Table 3. The study was divided into three parts. The first part of the study is a comparison between a transparent version of RADMC, NEQAIR, and actual experimental results[6] for three points along the trajectory of the Fire II vehicle using the Langley Upwind Relaxation Algorithm (LAURA) code[7] to obtain flowfield solutions. The

Table 3 Freestream conditions

Case	T_∞, K	P_∞, N/m^2	ρ_∞, kg/m^3	Altitude, km	V, km/s
Fire-1631 s	212	0.56	9.15×10^{-6}	84.6	11.37
Fire-1634 s	195	2.09	3.72×10^{-5}	76.4	11.36
Fire-1637.5 s	228	9.55	1.47×10^{-4}	67.1	11.25
AFE #1	189	0.31	5.68×10^{-6}	87.3	9.86
AFE #2	197	1.57	2.79×10^{-5}	77.9	8.91
AFE #3	200	2.64	4.29×10^{-5}	75.2	9.33

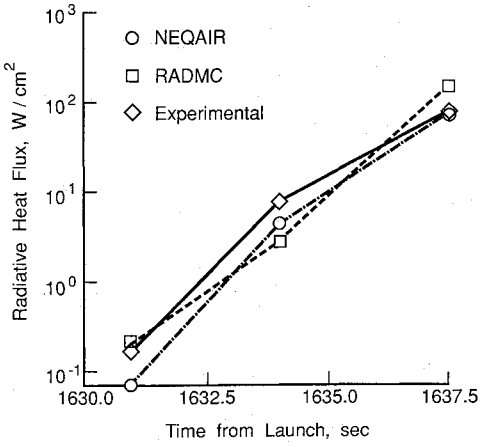

Fig. 2 Fire II radiative heat flux.

Table 4 Transparent radiative heating comparison in the visible and infrared spectral region

Case	Radiative heating, W/cm²		
	NEQAIR	RADMC	Experimental
Fire-1631 s	0.0699	0.1838	0.157
Fire-1634 s	4.271	2.711	7.30
Fire-1637.5 s	77.94	151.26	81.7
AFE #1	0.0310	0.0169	—
AFE #2	0.417	1.644	—
AFE #3	2.831	2.753	—

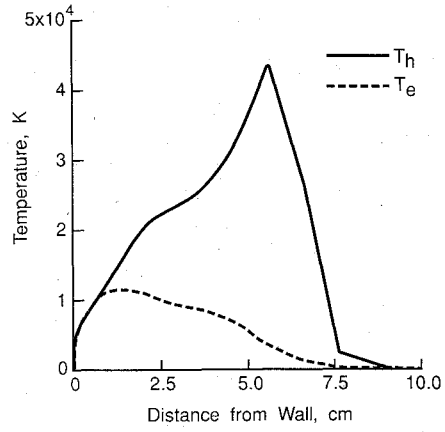

Fig. 3 Fire II stagnation temperature profile, 1634 s.

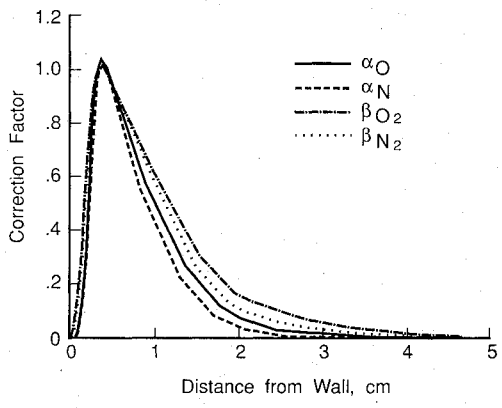

Fig. 4 Fire II correction factors, 1634 s.

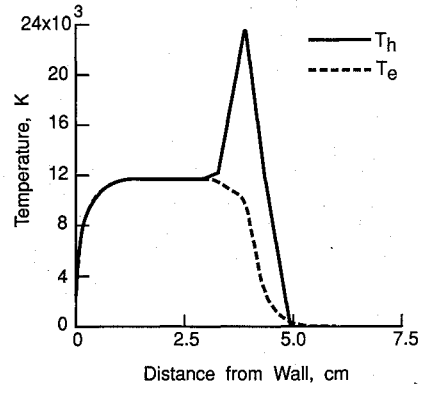

Fig. 5 Fire II stagnation temperature profile, 1637.5 s.

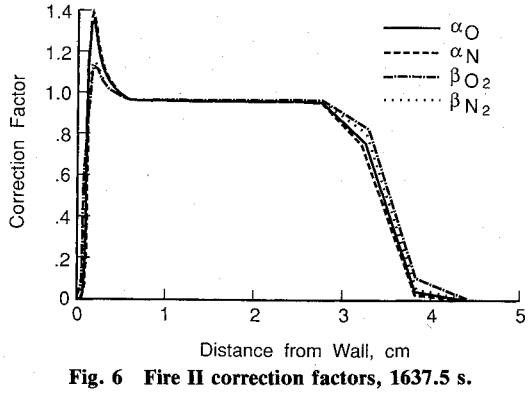

Fig. 6 Fire II correction factors, 1637.5 s.

second part is a comparison between RADMC and NEQAIR for three points typical of the proposed trajectory of the AFE using the flowfield solution method of Carlson et al.[1] The third part is an examination of the radiative heating of the AFE vehicle using the nongray version of RADMC with flowfield solutions obtained from the LAURA code. All radiation codes were run in an uncoupled fashion from the flowfield solution methods used.

Fire II Radiative Heating Comparison

The flowfield solutions obtained from the LAURA code for this comparison utilized the chemical kinetics of Park.[8] In addition, since the only radiometer data available from the Fire II flight were for wavelengths greater than 2,000 Å, NEQAIR's spectral range was left at its original 2,000–15,000 Å limits. NEQAIR's spectral resolution was increased from 5,000 to 20,000 points, however, to insure accurate results. The RADMC code ran in approximately one ten-thousandth of the computational time NEQAIR required for identical flowfields in all cases. RADMC and NEQAIR were then compared using a transparent gas version of the RADMC code for bands five and eight of the eight-step model (Table 2). Because of the low absorption in this portion of the spectrum, as shall be seen in subsequent sections, a transparent analysis is justified.

The radiative heating calculated by both codes for the Fire II vehicle is compared with the experimentally measured radiation in Fig. 2 and included in Table 4. Whereas NEQAIR yields radiative heating that is below the experimental values for the Fire II vehicle, RADMC shows variations both above and below the observed radiative heating. Despite the variation of both codes from the experimental values, both tend to show similar trends in radiative heating.

Temperatures and nonequilibrium correction factors for the 1634 s point along the Fire II trajectory are plotted in Figs. 3 and 4, respectively, and are typical of the first two points of the Fire II trajectory examined. Thermal nonequilibrium is significant throughout most of the shock layer. Furthermore, the nonequilibrium is apparent in the correction factors. The radiative heating at the surface obtained from NEQAIR is 4.271 W/cm² for the 2,000–15,000 Å region. RADMC yields a radiative heating of 2.711 W/cm².

At the 1637.5 s point of the Fire II flight, the flowfield changes character and becomes dominated by thermal equilibrium. The only thermal nonequilibrium observed in the flowfield is in the immediate postshock region (Fig. 5). At this point, the NEQAIR code, at 77.94 W/cm^2, was in exceptional agreement with the observed radiative heating from Fire II of 81.7 W/cm^2. By contrast, RADMC yielded a radiative heating of 151.26 W/cm^2. By inspecting the correction factors in Fig. 6, the correction factors through the radiating portion of the shock layer (Fig. 7) are approximately equal to one. These values indicate that only minor adjustments to the radiative cross sections were made, as would be expected in thermal equilibrium. It is reasonable then to assume that the discrepancy between RADMC and the NEQAIR computed values for radiative heating was caused by some influencing factor other than the nonequilibrium correction factors.

AFE Radiative Heating Comparison

The AFE flowfield solutions for the comparison were obtained from the AFE2 code modified by Carlson et al.[1] from an inverse method originally developed by Grose.[9] The AFE2 code uses the Modified Coupled Vibration Dissociation Vibration (MCVDV) model option with the chemical rates of Kang and Dunn.[10] Note that the present results are only intended to compare RADMC and NEQAIR, and for this comparison, a simplified inviscid code was used that assumes a Rankine-Hugoniot shock. These results should not be compared with the radiative heat-transfer calculations made for the AFE in other investigations or to those in the next section, which utilized more complete flowfield calculations. These results are only intended to be used in a comparison of RADMC with NEQAIR for an identical flowfield.

The comparison between RADMC and NEQAIR results for the three AFE trajectory points yielded reasonable agreement between the two codes (Table 4). The radiative intensities resulting from RADMC and NEQAIR calculations are presented in Fig. 8 for the third AFE point, and the corresponding temperature profile is presented in Fig. 9. The patterns exhibited in Figs. 8 and 9 can be considered typical for all three AFE points. Although specific radiative intensity profiles do not match, general intensity patterns are similar.

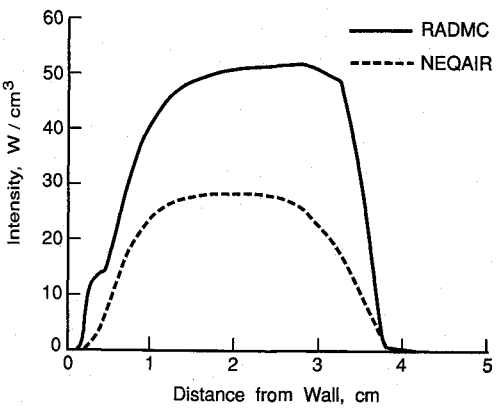

Fig. 7 Fire II stagnation radiative intensity, 1637.5 s.

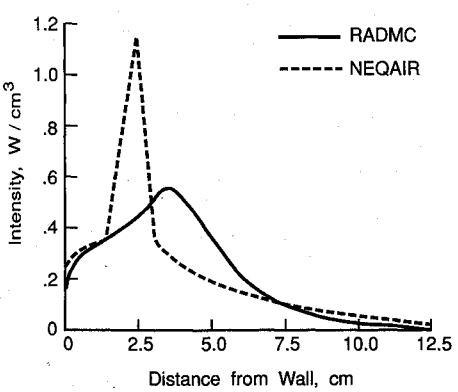

Fig. 8 AFE #3 stagnation radiative intensity.

AFE Radiative Heating

Two typical AFE flowfields (AFE #1 and AFE #2) were obtained from the LAURA code using the chemical kinetics of Kang and Dunn.[10] Both the transparent and nongray versions of RADMC were used to study the radiative heating along the stagnation streamline for both flowfields, and the results are presented in Table 5. Bands 5 and 8 of the eight-step model roughly correspond to the visible and infrared portions of the spectrum; bands 6 and 7 are the ultraviolet line wings and line centers, respectively. Bands 1-4 represent the vacuum ultraviolet portion of the spectrum (Table 2).

At AFE #2, both the nongray and transparent version of RADMC yielded a radiative heat transfer for the visible and infrared portions of the spectrum of 5.26 W/cm^2, which compares well with the 6.63 W/cm^2 result of Park[8] and the 5.94 W/cm^2 result of Candler[11] for similar freestream conditions. However, the AFE #1 result of 1.435 W/cm^2 for the same spectral region was high compared with the 0.112 W/cm^2 value obtained by Candler for similar freestream conditions. The three-temperature model in the flowfield solution method used by Candler could possibly account for this discrepancy, but any comparison between a two-temperature and a three-temperature model is out of the scope of the current study. However, the transparent RADMC results for AFE #1 are in reasonable agreement with the 0.93 W/cm^2 result for the visible and infrared spectrum calculated by Moss and Price[12] at 90-km altitude. Moss and Price also calculated a total transparent radiative heat transfer of 2.28 W/cm^2 at this same trajectory point, as compared with the total transparent flux of 3.498 W/cm^2 obtained from RADMC.

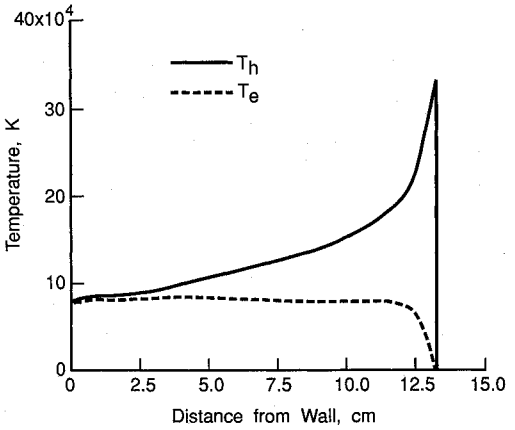

Fig. 9 AFE #3 stagnation temperature profile.

Table 5 Transparent and nongray radiative heating at two AFE points utilizing the eight-step model

	Radiative heating, W/cm^2			
	AFE #1		AFE #2	
Band	Transparent	Nongray	Transparent	Nongray
1	1.344	0.1211×10^{-3}	3.234	0.2340×10^{-4}
2	0.0738	0.0434	0.1812	0.0661
3	0.1421	0.1159	0.3432	0.2364
4	0.0431	0.0421	0.0977	0.0925
5	0.6080	0.6080	2.0280	2.0280
6	0.2783	0.2783	0.7042	0.7042
7	0.1834	0.1449×10^{-5}	0.4981	0.1908×10^{-3}
8	0.8261	0.8261	3.2290	3.2290
Total	3.499	1.914	10.3200	6.3560

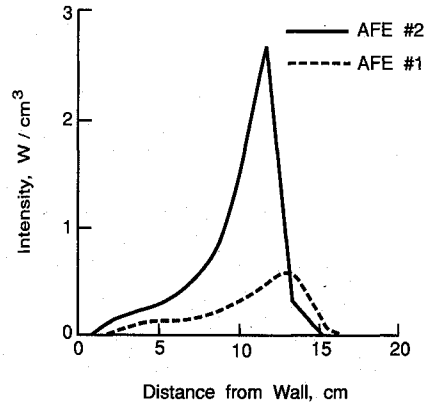

Fig. 10 Stagnation radiative intensity for AFE trajectory points.

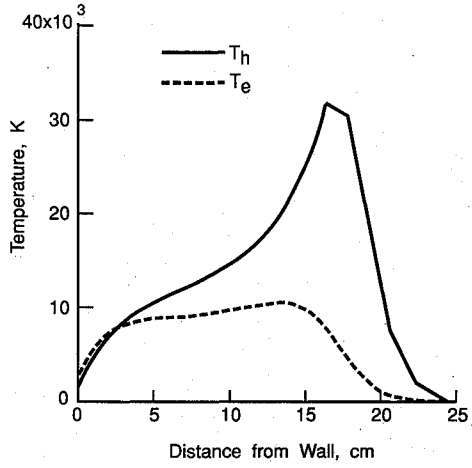

Fig. 11 AFE #1 stagnation temperature profile.

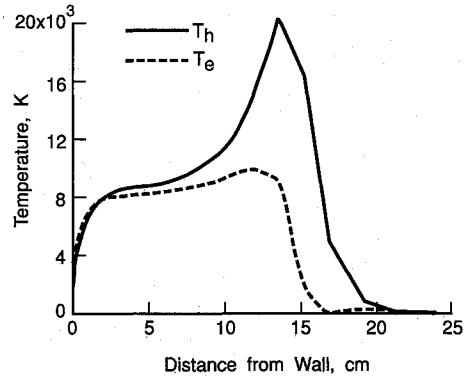

Fig. 12 AFE #2 stagnation temperature profile.

A comparison between the transparent and nongray results for the two AFE points indicates that, despite the differences in the freestream conditions between the two points, the percentage of radiation absorbed remained fairly constant for each region of the spectrum. As would be expected, the vacuum ultraviolet and ultraviolet regions were highly absorbed in both cases, with the total vacuum ultraviolet radiation absorbed being approximately 90% of the total emission for both cases. The ultraviolet radiation is 40% absorbed, with all the absorption taking place in the line centers, and the line wings remain virtually unabsorbed. The visible and infrared portions of the spectrum remained transparent throughout both shock layers.

The stagnation streamline radiative intensitives for both AFE points are presented in Fig. 10, where no deviations from expected patterns are indicated. Temperature profiles for both

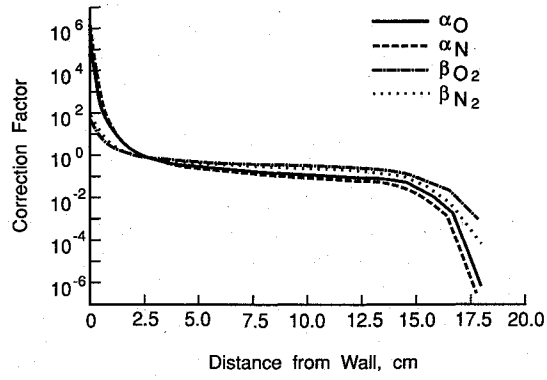

Fig. 13 AFE #1 correction factors.

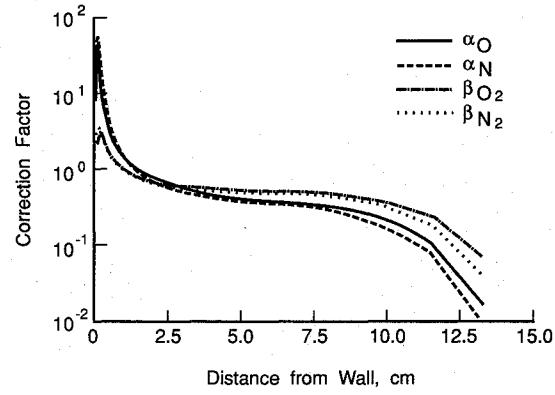

Fig. 14 AFE #2 correction factors.

points are presented in Figs. 11 and 12. The LAURA code results for both AFE trajectory points indicate that the electron temperature (which is again assumed to be equal to the vibrational temperature of N_2) exceeds the heavy particle translational temperature in the boundary layer. The correction factors (Figs. 13 and 14) conform to expected patterns for these flowfield solutions in that they are significantly below one in the immediate postshock region of the flow where particle excitation would be expected to lag equilibrium values since $T_e < T_h$. In the boundary layer, where $T_e > T_h$, particle excitation exceeds that predicted by equilibrium values at the local heavy particle temperature. The excitation enhancement in this region has little influence on the actual radiative intensity, since it occurs where both T_e and T_h are small enough that the radiation is minimal.

Concluding Remarks

A simplified method for the calculation of nonequilibrium radiative heat transfer has been obtained and applied to AFE and Fire II flowfields. During the course of this investigation, several interesting phenomena were observed. First, while the vacuum ultraviolet portion of the spectrum (VUV) and ultraviolet portion of the spectrum (UV) portions of the spectrum were highly absorbed in all flowfields, a significant amount of radiative flux in this spectral region was transferred to the surface of the AFE vehicle. In addition, particle excitation in the boundary layer exceeded the levels predicted by equilibrium calculations because the electron temperature exceeded the heavy particle translational temperature for this part of the flowfield. However, none of the computational difficulties observed in the boundary layer by the previous correction factor method appeared in any of the cases studied, and calculated excitation patterns conformed to expected trends throughout the shock layer whether the shock layer was dominated by nonequilibrium effects or not. It was also noticed that the various assumptions of differing flowfield solution methods strongly influenced the radiative heat transfer

calculations, and work will continue on determining the most appropriate assumptions for accurate radiative heat transfer computations.

The correction factor approach to the solution of uncoupled nonequilibrium radiative heat transfer using an equilibrium air radiation model appears to yield reasonable trends and magnitudes for most of the flowfields studied, and requires little computational time. The potential time savings compared with detailed models would not only speed uncoupled engineering studies, but would greatly reduce the overall computational time were RADMC coupled to a flowfield solution method in the future. However, it is important to note that radiative processes in both thermal and chemical nonequilibrium are not completely understood at the present time, and the method described in this paper should be considered an approximate engineering method.

Acknowledgments

The preceding study was sponsored in part by NASA Contract NAS1-18599. The authors wish to thank the Technical Monitor, Dr. Kenneth Sutton, for his support and Dr. Peter Gnoffo for providing the LAURA flowfield solutions used in this report. The comments of Jim Jones of Analytical Mechanics Associates and Dr. Leland Carlson of Texas A&M University were also greatly appreciated.

References

[1]Carlson, L. A., Bobskill, G. J., and Greendyke, R. B., "Comparison of Vibration Dissociation Coupling and Radiative Heat Transfer Models for AOTV/AFE Flowfields," AIAA Paper 88-2673, June 1988.

[2]Jones, J. J., "The Rationale for an Aeroassist Flight Experiment," AIAA Paper 87-1508, June 1987.

[3]Greendyke, R. B., "A Parametric Study of Shock Jump Chemistry, Electron Temperature, and Radiative Heat Transfer Models in Hypersonic Flows," Masters Thesis, Texas A&M Univ., College Station, TX, Aug. 1988.

[4]Olstad, W. B., "Nongray Radiating Flow about Smooth Symmetric Bodies," *AIAA Journal,* Vol. 9, Jan. 1971, pp. 122–130.

[5]Park, C., "Nonequilibrium Air Radiation (NEQAIR) Program: User's Manual," NASA TM-86707, July 1985.

[6]Cauchon, D. L., "Radiative Heating Results from the Fire II Flight Experiment at a Reentry Velocity of 11.4 Kilometers per Second," NASA TMX-1402, July 1967.

[7]Gnoffo, P. A., "Upwind-Biased, Point-Implicit Relaxation Strategies for Viscous, Hypersonic Flows," AIAA Paper 89-1972, June 1989.

[8]Park, C., "Assessment of Two-Temperature Kinetic Model for Ionizing Air," AIAA Paper 87-1574, June 1987.

[9]Grose, W. L., "A Thin Shock Layer Solution for Nonequilibrium, Inviscid Flows in Earth, Martian, and Venusian Atmospheres," NASA TND-6529, Dec. 1971.

[10]Kang, S. W., and Dunn, M. G., "Theoretical and Measured Electron Density Distributions for the RAM Vehicle at High Altitudes," AIAA Paper 72-689, June 1972.

[11]Candler, G., and Park, C., "The Computation of Radiation Nonequilibrium Hypersonic Flows," AIAA Paper 88-2678, June 1988.

[12]Moss, J. N., and Price, J. M., "Direct Simulation of AFE Forebody and Wake Flow with Thermal Radiation," NASA TM-100673, Sept. 1988.

Ernest V. Zoby
Associate Editor